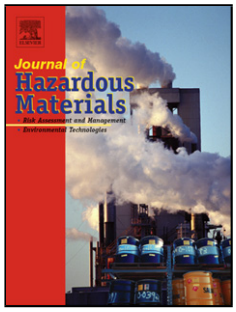

Title: ACCLIMATION OF *Tetrahymena thermophila* TO BULK AND nano-TiO_2 PARTICLES BY CHANGES IN MEMBRANE FATTY ACIDS SATURATION

Authors: K. Rajapakse, D. Drobne, J. Valant, M. Vodovnik, A. Levart, R. Marinsek-Logar

PII: S0304-3894(12)00420-7
DOI: doi:10.1016/j.jhazmat.2012.04.029
Reference: HAZMAT 14174

To appear in: *Journal of Hazardous Materials*

Received date: 7-11-2011
Revised date: 31-3-2012
Accepted date: 13-4-2012

Please cite this article as: K. Rajapakse, D. Drobne, J. Valant, M. Vodovnik, A. Levart, R. Marinsek-Logar, ACCLIMATION OF *Tetrahymena thermophila* TO BULK AND nano-TiO_2 PARTICLES BY CHANGES IN MEMBRANE FATTY ACIDS SATURATION, *Journal of Hazardous Materials* (2010), doi:10.1016/j.jhazmat.2012.04.029

ACCLIMATION OF *Tetrahymena thermophila* TO BULK AND nano-TiO_2 PARTICLES BY CHANGES IN MEMBRANE FATTY ACIDS SATURATION

K. Rajapakse[a] katarina.ales@bf.uni-lj.si**, D. Drobne**[b,c,d] damjana.drobne@bf.uni-lj.si**, J. Valant**[b] janez.valant@bf.uni-lj.si**, M. Vodovnik**[a] masa.vodovnik@bf.uni-lj.si**, A. Levart**[a] alenka.levart@bf.uni-lj.si**, R. Marinsek-Logar**[a*] romana.marinsek@bf.uni-lj.si

[a]Department of Animal Sciences, University of Ljubljana, Groblje 3, SI-1230 Domzale, Slovenia Fax: +38617241005

[b]Department of Biology, University of Ljubljana, Vecna pot 111, SI-1000 Ljubljana, Slovenia

[c]Centre of Excellence in Advanced Materials and Technologies for the Future (CO NAMASTE), Jamova 39, SI-1000 Ljubljana, Slovenia

[d] Centre of Excellence in Nanoscience and Nanotechnology (CO Nanocenter), Jamova 39, SI-1000 Ljubljana, Slovenia

Department of Animal Sciences, University of Ljubljana, Groblje 3, SI-1230 Domzale, Slovenia, Fax: +38617241005

Highlights

T. thermophila was exposed to TiO_2 particles at sub-toxic concentrations.

Exposure to TiO_2 particles resulted in changed cell membrane in fatty acid profile resulting in increased membrane rigidity.

Altered cell membrane composition is not accompanied by lipid peroxidation or ROS elevation.

Particles were detected in food vacuoles where filling and subsequent release was followed.

Abstract

We provide experimental evidence that changes in the membrane fatty acid profile of *Tetrahymena thermophila* incubated with nano- or bulk TiO_2 particle are not accompanied by ROS generation or lipid peroxidation. Consequently these changes are interpreted as acclimation to unfavorable conditions and not as toxic effects. *T. thermophila* cells were exposed to TiO_2 particles at different concentrations for 24 hours at 32ºC. Treatment of cultures with nano- and bulk TiO_2 particles resulted in changes of membrane fatty acid profile, indicating increased membrane rigidity, but no lipid peroxidation or ROS generation was detected. There were no differences in membrane composition when *T. thermophila* was exposed to nanosized or bulk-TiO_2 particles. We also observed reversible filling of food vacuoles, but this was different in case of nano- or bulk TiO_2 exposure. Our results suggest that interactions of particles and cell membranes are independent of oxidative stress.

Keywords: TiO_2 nanoparticles, acclimation, membrane fatty acid profile, *Tetrahymena thermophila*, food vacuoles.

ABBREVIATIONS

Nutrient rich medium; RM

Nutrient poor medium; PM

INTRODUCTION

There have been many studies on the effects of nanosized TiO_2 (nano-TiO_2) on aquatic and terrestrial organisms [1] [2]. The most frequently studied consequences of exposure to nano-TiO_2 are cytotoxicity and genotoxicity *via* oxidative stress [3] [4].

Irrespective of the exposure route, the first contact between the cells and nanoparticles must involve the cell membranes [5]. Accordingly, we investigated whether a suspension of TiO_2 particles could affect the cell membrane composition of a eukaryotic microorganism *Tetrahymena thermophila* in the absence of light (when ROS generation due to catalytic activity of TiO_2 was expected to be minimized) and whether this is evidence of a toxic response or of acclimation to unfavourable environmental conditions. A significant decrease in membrane fluidity after exposure of *Tetrahymena sp.* to TiO_2 has already been documented [6] [7].

There are numerous reports on functional alterations of cell membranes occurring under unfavourable environmental conditions involving for example, temperature or chemicals. Bearden *et al*. (1999) [8] and Shultz *et al*. (2002) [9], described membrane fatty acid profile alterations in *Tetrahymena sp.* resulting from exposure to chemicals such as pentachlorophenol and 1-octanol, acting noncovalently. Shug *et al.* (1969), [10] detected a marked effect of iron ions on the desaturation of fatty acids in the membrane of *T. thermophila*. When exposed to methyl mercury, small but distinct changes in the profile of membrane fatty acids were detected (personnel communication) and it was suggested that profiling of fatty acid methyl esters (FAME-s) could be used for identification of different groups of chemicals in *T. thermophila*. The study of effects of an aqueous suspension of fullerene (C60) on bacteria also showed changes in lipid composition which were dependent on the C60 concentration [11]. The same authors also successfully employed profiling of FAME-s. Alterations in membrane lipid profiles have been interpreted as a physiological adaptation or an acclimation to extreme conditions [10] [12] [13, 14]. Mortimer *et al.* [7] demonstrated changes in the fatty acid profile of protozoon *T. thermophila* exposed to nano-CuO.

Functional alterations of cell membranes could also be interpreted as acclimation to unfavorable conditions. However, acclimation is not linked only to membranes. This phenomenon acclimation has

been defined as a short-term phenotypic change, which allows survival in suboptimal environmental conditions, including pollution [8, 15, 16]. When suboptimal conditions result from exposure to chemicals, the primary stress response of an organism compensates for the potential adverse effects on cells, but with elevated concentrations of chemicals and prolonged exposure to them, toxic effects are unavoidable. An association of alterations in membrane structure with cytotoxicity has been reported by Clarke *et al*., (1990) [17] for human breast cells and also by Mortimer *et al*., (2011) [7] for *T. thermophila*. So far, *T. pyriformis* has been shown when exposed to temperature changes, to respond through changes in membrane fatty acid profiles [15] and to organic chemicals considered to act *via* a nonpolar toxic action [16] [8]. Very recently, changes in membrane lipid composition in terms of lowering membrane fluidity were demonstrated by Mortimer *et al*., (2011) [7] and explained as an adaptation mechanism to exposure to CuO nanoparticles [7]. These authors studied the effects of toxic concentrations of nano-CuO on the membrane of *T. thermophila* [7].

The aim of this research was to assess the total membrane fatty acid profile of *T. thermophila* after exposure to TiO_2 particles in a range of concentrations. Organisms were exposed to particles *via* food as well as substratum. In parallel experiments, some additional biomarkers such as lipid peroxidation, ATP concentration, cell morphology and filling of particles in vacuoles were analyzed in an attempt to correlate changes in membrane fatty acid saturation with potential cytotoxic effects. The effects of nano- and bulk TiO_2 particles were compared. We hypothesize that if changed membrane fatty acid profile of *T. thermophila* exposed to TiO_2 particles is not accompanied by a cytotoxic response this is direct evidence of acclimation to the particles present in media and not an indication of particle toxicity.

1 MATERIALS AND METHODS

1.1 Chemicals.

All reagents were purchased from Sigma Aldrich Co (St. Louis, MO, USA), Merck (Darmstadt, Germany) or Biolife (Milan, Italy), unless specifically stated otherwise.

1.2 T. thermophila growth and exposure conditions.

Axenic cultures of *T. thermophila* from the Protoxkit F^{TM} (MicroBioTests Inc.) were grown for 24 h in the dark at 32°C in a semidefined proteose-peptone based medium [18] - a nutrient rich medium; RM. The nutrient rich medium contains 5 g D-glucose, 5 g proteose-peptone, 1 g yeast extract, 1.2 g Trisma-base, chlorides (2.28 µM $CaCl_2.2H_2O$, 0.29 µM $CuCl_2.2H_2O$, 0.05 µM $FeCl_3.6H_2O$, 0.03 µM $MnCl_2.6H_2O$, 0.004 µM $ZnCl_2$) and sulphates (4.1 µM $MgSO_4.7H_2O$, 0.64 µM $Fe(NH_4)_2(SO_4)_2.6H_2O$), up to 1000 ml doubly distilled H_2O, pH corrected to 7.35 with HCl. The cell density obtained in these culture conditions was approximately 10^5 cells/ml.

The cells were harvested by centrifugation (3 min, 60 rcf), washed and resuspended in a medium specifically modified for this experiment: semidefined proteose-peptone based medium by Schultz (1997) [18] lacking yeast extract and bacteriological peptone - a nutrient poor medium; PM. This nutrient poor medium contains 5 g D-glucose, 1.2 g Trisma-base, 1000 ml doubly distilled H_2O. The pH of the medium was adjusted to 7.4 with HCl and temperature was held constant at 32°C for the entire experiment. All experiments were performed in batch cultures of 100 ml in Erlenmeyer flasks, and aerated by shaking (90 rpm) in darkness.

After 24 h in the PM, cells were treated with bulk or nano-TiO_2. The final concentrations of particles in the medium were: 0.1, 1, 10, 100, 1000 µg/ml. Following the addition of TiO_2, *T. thermophila* cultures were incubated at 32.0°C for 48 h. Assays of ATP concentration, total protein concentration, filling of vacuoles with TiO_2 and morphological characterizations were performed at several time intervals (Fig. 1). For each concentration of nano- or bulk TiO_2, three independent assays were carried

out. A supplementary set of three replicates, without TiO_2 particles, was set up for each assay as a control.

1.3 Bulk and nano-TiO_2 tested suspension.

The TiO_2 nanoparticles were supplied in the form of a powder with guaranteed 99.7% purity having the following characteristics provided by the manufacturer: Anatase crystalline structure; average particle size 15 nm; and surface area, 190 to 290 m^2/g. Bulk and nano-TiO_2 particles were dispersed in PM using bath sonication for 30 min.

The dispersions of nanoparticles (1000 µg/ml) were inspected by dynamic light scattering (DLS) using a 3D DLS-SLS (dynamic light scattering - static light scattering spectrometer; LS Instruments, Fribourg, Switzerland). This allows the determination of hydrodynamic radii of particles in extremely turbid suspensions by a so-called 3D cross-correlation technique that successfully eliminates multiple scattering of light. As the light source a HeNe laser operating at a wavelength of 632.8 nm was used. Scattering was measured at an angle of 90°.

Zeta potentials of nano-TiO_2 suspensions (1000 µg/ml) were measured with ZetaPals, (Brookhaven Instrument Corporation) in the PM medium, and used to assess the exposure to living cells. Zeta potentials were measured at different pH values, adjusted by adding NaOH or HCl to the suspension.

1.4 Assessment of cellular fatty acid composition by gas chromatography.

T. thermophila cells were harvested by centrifugation, pellets were resuspended in sterile doubly distilled water (1 ml), frozen at -20 °C and then lyophilized. Dried samples were pulverized and transferred to HACH screw cap test tubes. First, the sample was mixed with hexane (0.5 ml) and then 1.5M HCl in MeOH (1 ml) and pure MeOH (1ml) were added. The test tubes were filled with N_2 and

incubated at 80°C for 10 min. The reaction was stopped by cooling the tubes in ice. Following the addition of doubly distilled water (2 ml), each reaction mixture was vigorously mixed for 1 min and centrifuged (30s, 670 rcf). The organic phase containing FAMES extracted in hexane was transferred to a clean vial and filled with N_2. The samples were stored at –20 °C until analysis.

Fatty acid methyl esters (FAME-s) were separated by capillary gas chromatography using Omegawax TM 320 (30m x 0.32 mm ID x 0.25 mm) capillary column with polyethylene glycol as the stationary phase. Helium was used as a carrier gas with a flow rate of 2.0 ml/min, and a split ratio of 10:1. The initial temperature for analysis was 185°C and the final temperature was 215°C with a temperature increase rate of 1°C/min. The run time was 54 min and volume injected was 2 µl. Identification of fatty acid methyl esters was achieved by comparison of retention times and results were calculated using response factors derived from chromatographic standards of known composition (Nu Chek Prep, GLC-85, Nu-Chek Prep Inc., Elysian, USA). The gas chromatography system used was an Agilent 6890 series GC equipped with Agilent 7683 Automatic Liquid Sampler, 7683 Injector and FID detector.

Results were analyzed using ChemStation Plus® software. Membrane fatty acids which were present as less than 0.5% of total fatty acids were designated as “trace fatty acids” and were not considered further. The data were analyzed statistically applying Student`s t-test with significance level of 0.05.

1.5 Assessment by MDA measurement of the extent of lipid peroxidation.

Lipid peroxidation was measured as the formation of malondialdehyde (MDA) in *T. thermophila* samples at 32°C after 0, 4 and 24 h of incubation [19]. Cells were homogenised and total protein concentration was measured spectrophotometrically at 280 nm, and used as a measure of biomaterial in the experiments. For measurement of MDA concentration, 500 µl of homogenised sample was

mixed with 500 ml of buffer A (30% trichloroacetic acid, 0.75% 2-thiobarbituric acid, 0.5 M HCl and 0.02% butylated hydroxytoluene), incubated at 90°C for 30 min, then chilled on ice. n-Butanol (1.5 ml) was mixed with the sample and centrifuged (10 min, 6700 rcf). The absorbance of the resulting chromophore was measured at 535 nm and 600 nm. The latter was subtracted from the former to correct for nonspecific turbidity. The concentration of MDA was calculated using an extinction coefficient of 156 mM^{-1} cm^{-1} [19]. For statistical analysis, each concentration of MDA was divided by the total protein concentration of the corresponding sample.

1.6 Viability assessment by ATP assay.

Adenosine 5'-triphosphate (ATP) Bioluminescent Assay Kit (Sigma Aldrich, Germany) was employed for the quantitative bioluminescent determination of ATP. For ATP extraction, protozoa culture samples (100 µl) were added to boiling extraction buffer (900 µl), as described previously [20], 0.1M Tris and 2mM EDTA were added and the pH was adjusted to 7.8 with acetic acid [21]. The relative light units (RLU) were recorded in JUNIOR LB 9509 (Berthold technologies). The ATP concentration (measured in µmol ATP/l) was calculated using the equation:

$$[ATP]= 10^{(\log RLU-b)/a} * 10$$

where a and b are factors calculated from the calibration curve with a correlation coefficient R=0.99.

1.7 Assessment by light microscope of percentage of T. thermophila cells containing at least one vacuole filled with TiO_2.

Total and dead cell numbers were estimated by conventional direct microscopic counting under observation at 200 times magnification in a Neubauer chamber. The uptake of TiO_2 by food vacuoles (Fig. 2) was studied from two perspectives: treatment with several TiO_2 exposure concentrations (at

0.1, 1, 10, 100, 1000 µg TiO_2/ml) and with different time exposures (0, 1, 2, 4, 24, 48 h). A 10 µl sample of culture was put into a Neubauer chamber, and dead cells, including non-motile cells and cells with changed morphology were counted, then 5 µl of 4% formalin was added to kill the cells and a total cell count was performed.

The percentage of cells containing at least one food vacuole filled with TiO_2 particles was calculated as follows:

Vacuole formation (%) = number of cells containing at least one TiO_2 vacuole/100 cells.

2 RESULTS

2.1 Characteristics of TiO_2 nanoparticle suspensions.

The primary and secondary characteristics of the nanoparticles used in the experiments were assessed. Primary characteristics include particle size, shape and crystallinity and have been described previously and the same particles were used in the current experiments [22]. Secondary characteristics are those of nanoparticles in a suspension. In our study, particles were suspended in nutrient poor medium (PM) and analysed. DLS analysis showed that the average value of the hydrodynamic radius of TiO_2 nanoparticles suspended in test medium was 820 nm. The average particle size of bulk TiO_2 could not be accurately measured by this approach because of the presence of many larger agglomerates.

Zeta potentials of TiO_2 nanoparticle suspension (1000 µg/ml) were measured in the same medium used to expose cells, at different pH values. The Zeta potential recorded at pH 7.4 was -15 mV, which is equivalent to a suspension of incipient stability (Fig. 3).

2.2 Cellular fatty acid composition (FAME-s).

A 24 h exposure of *T. thermophila* to TiO_2 at 32°C resulted in differences of relative percentages of straight chain saturated, monounsaturated, saturated *iso* and *ante-iso* fatty acids in cell membranes of *T. thermophila* between TiO_2 treated populations and controls (Table 1). A significant increase of straight chain saturated fatty acids in membrane cell lipids was detected in exposed cells (Fig. 4). The increase of saturated fatty acids was mostly due to the increase of 15:0, 16:0, 17:0 and 18:0 fatty acids (data not shown). All these changes were independent of TiO_2 size (nano- or bulk) and exposure concentration (0.1, 10, 1000 μg TiO_2/ml) but compared to control cells, the proportions of unsaturated fatty acids remained unchanged (Fig. 4).

A certain proportion of saturated membrane fatty acids has a branched-chain structure, which exist in either *iso* or *ante-iso* forms. These two isoforms are known to differ in their influence on membrane fluidity, and consequently we further analyzed the potential association between the relative amount of each branched-chain isomer and the exposure conditions. The results showed that both isoforms were decreased in cells exposed to bulk or nanoTiO_2 (*iso* mostly on account of 15:0 *iso* and 16:0 *iso* fatty acids) in comparison to controls, regardless of the concentration (data not shown). However, the decrease in *ante-iso*- saturated fatty acids was much more pronounced (Fig. 5), mostly on the account of 15:0 *ante-iso* fatty acid (data not shown).

Another difference between controls and TiO_2-treated populations of *T. thermophila* was in the average length of membrane fatty acids (Table 1). An increase in the average length of fatty acids from 15.3 C atoms in control samples to 16.0, 15.9 and 15.5 in cultures treated with bulk TiO_2 in exposure concentrations of TiO_2 of 0.1, 10, 1000 μg TiO_2/ml respectively, was noted. An increase to 16.1, 16.2 and 16.0 C atoms in nano-TiO_2 treated cultures (in exposure concentrations of TiO_2 of 0.1, 10, and 1000 μg TiO_2/ml respectively, was detected (Table 1). Thus, the lipid bilayer in cultures exposed to TiO_2 particles appears, in comparison to controls, to be wider [23], namely from 0.2 to 0.7 C atoms in cultures treated with bulk TiO_2 and from 0.7 to 0.9 C atoms in nano-TiO_2 treated cultures.

2.3 Lipid peroxidation.

When *T. thermophila* is exposed to TiO_2, elevation of the amount of MDA, compared to controls, is not detected. The average content of MDA in the control sample is 140 ± 23 nM of MDA per mg of protein.

2.4 ATP concentration in T. thermophila cultures.

When *T. thermophila* is exposed to bulk or nano- TiO_2 for 24 h, no significant alterations in ATP could be observed. ATP concentrations were similar to that measured in controls (Fig. 6).

2.5 Filling of vacuoles with TiO_2.

Filling of vacuoles with dense material was observed in cells exposed to nano- or bulk TiO_2 present in the media at concentrations higher than 10 µg/ml. At concentrations of TiO_2 particles below 10 µg/ml and in control samples, no vacuoles filled with dark material were observed.

Significant differences were observed in the proportion of cells containing vacuoles filled with TiO_2 that were exposed to bulk TiO_2 as opposed to nano-TiO_2. *T. thermophila* cells exposed to bulk TiO_2 contained a higher percentage of vacuoles filled with TiO_2 than those exposed to nano-TiO_2. This was recorded at all observation times throughout the experiment (Fig. 7). A relatively small amount (< 5%) of cells containing vacuoles filled with TiO_2 was observed after 24 h compared to those exposed for 1, 2 or 4 h at the highest exposure concentrations of bulk and nano-TiO_2 indicates clearing of *T. thermophila* after 24 h (Fig. 7).

2.6 Morphological alterations characteristics of T. thermophila.

In investigated samples of *T. thermophila* treated with, bulk or nano-TiO_2, the type of cell rupture as described previously by Dai *et al*. (2008) [24] was observed. The proportion of ruptured cells in all experiments was between 0% and 5%. The pattern of cell rupture was not related either to particle exposure concentration, or to the duration of exposure. These cells were enlarged, round shaped and vacuoles appeared more pronounced. The oral apparatus was disrupted and formed a large vacuole, from which the content of cells leaked. This phenomenon was not observed in control samples.

Further, we did not observe either normal or abnormal mature resting cysts in cultures exposed to nano-or bulk TiO_2, as some authors have reported in stress conditions for ciliates [24].

3 DISCUSSION

Our results showed that exposure of *T. thermophila* to nano-TiO_2 or bulk TiO_2 in a range of exposure concentrations of 0.1, 10, and 1000 μg/ml caused changes in membrane lipid composition but no differences in ROS concentration or lipid peroxidation. Since changes in membrane lipid composition were not correlated with toxicity markers they are interpreted as acclimation to unfavourable conditions, in this case the presence of TiO_2 particles in the medium. However, in groups exposed to either nanoparticles or bulk TiO_2, up to 5% of ruptured cells were observed. Ruptured cells were never observed in control populations. Obviously, for a certain small portion of cells, TiO_2 particles caused destruction.

We were able to detect the effects of TiO_2 particles on cells before toxic responses occurred. Both nano- and bulk TiO_2 caused significant decrease in the ratio of unsaturated to saturated straight chain fatty acids. Further, a significant decrease in percentage of *iso* and *ante-iso* branched fatty acids in cultures treated with nano- and bulk TiO_2 (Fig. 5) was detected. Both structural and geometrical isomers of fatty acids are known to affect membrane fluidity [25] and modes of modulation of membrane fluidity by inducing changes in fatty acid isomerisation are well known for bacteria exposed to extreme environmental conditions [26] [27]. Our results are in line with these findings where for example, a decrease of ante-isoforms is reported to lead to a decrease in the fluidity of membranes.

Changes in membrane composition leading to its increased rigidity have been reported often and associated with acclimation to suboptimal environmental conditions, such as rise in temperature [25] [28], hyperosmotic stress [29], particles and UV light [6] as well as nanoparticles [7]. Most authors report, that cell membrane rigidity is accompanied by lipid peroxidation [30]. Consequently, it is difficult to differentiate whether the response is acclimation to suboptimal conditions or a result of their adverse effect. In the current study, we succeeded in documenting membrane lipid changes in the

absence of any lipid peroxidation. In this way, we were able to confirm that changes in membrane lipid composition represent an acclimation to incubation of cells with both nano- and bulk particles. In our study no lipid peroxidation was detected in cultures with increased membrane rigidity. Observed membrane changes associated with TiO_2 particles and resulting in increase of membrane rigidity. In our experiments the choice of temperature was based on literature data, where optimal growth temperature for *T. thermophila* in the semidefined proteose-peptone based medium is 32°C [18] [31]. Growth of *T. thermophila* at the temperature selected is accompanied by *de novo* fatty acid synthesis, which is necessary in the type of membrane acclimation observed. The degree of change in membrane composition associated with the increase in rigidity indicated was not dose-dependent in relatively wide concentration range, from 0.1 μg/ml to 1000 μg/ml.

In published studies, different mechanisms of interaction between nanoparticles and cell membranes have been proposed. Hussain *et al*. (2005) [32] report that cell membranes associate with nanoparticles, some of which are internalized by the cells. Sayes *et al.* (2008) [33] interprets the affected cell membrane stability (lactate dehydrogenase release) and the decrease in mitochondrial membrane potential, assessed by the MTT method, after nanosized TiO_2 exposure as symptoms of 'leaky membranes', a mechanism in which cytoplasmic membrane rupture is a possible defence mechanism/strategy in case of overload concentrations of particles. Other authors explain disruption of membrane structures and stability either as a result of direct physical interactions between particles and membranes [5] or as a result of lipid peroxidation, itself a consequence of oxidative stress provoked by particles [34] [35]. Our results provide evidence that the interactions between TiO_2 particles and *T. thermophila* are independent of oxidative stress.

Ingested particles were observed in food vacuoles where the percentage of cells containing at least one vacuole filled with TiO_2 recorded at exposure concentrations 10, 100 and 1000 μg TiO_2/ml was dose- and time-dependent (Fig. 7). However, the amount of dense material in vacuoles failed to correlate with the detected membrane effect or alter ATP or protein concentration. This suggests that ingestion of nanoparticles and their sequestration into vacuoles does not pose a serious threat to the organism at

exposure concentrations up to 1000 μg/ml and exposure times of up to 48 h. Mortimer *et al.* (2010) [36] observed a more rapid uptake by *T. thermophila* of CuO nanoparticles than bulk CuO particles. This is not consistent with our results, where the uptake was higher for the bulk form when compared with equal exposure concentrations of nano-TiO_2. The CuO particle uptake reported by Mortimer *et al.* (2010) [36] was also much faster (requiring only four h) when compared to uptake of TiO_2, and further, in our study, cells were never completely filled with particles as they were in the CuO study.

We observed clearing of vacuoles filled with TiO_2 after 24 h of exposure. There are no similar previous reports on nanoparticle ingestion and clearing by protozoa, and we consider clearing to be a phase of feeding activity. Initially, a high percentage of cells containing at least one TiO_2-filled vacuole is observed and subsequently, almost no cells are observed containing food vacuoles filled with TiO_2. This clearance is then followed by another intense period of ingestion (Fig. 7). The increase of percentage of cells containing at least one food vacuole filled with TiO_2 (after 0, 1, 2, 4, 24, 48 h) correlated with increased particle concentration in the media (aggregate size and amount 10, 100, 1000 μg TiO_2/ml) (Fig. 7). The presence of particles in the food vacuoles indicates an exposure route of cells, in addition to the body surface, to nanoparticles.

We used a modified exposure medium for *T. thermophila* in order to reduce the effects of media on nanoparticle behaviour. The exposure media for *T. thermophila* was modified in order to reduce interactions between nanoparticles and biological media, TiO_2 toxic buffering with organic compounds and ions in media, but it still provided satisfactory energetic conditions for avoidance of starvation and competition for food. Murdock *et al*. (2007) [37] showed that particle size changed dramatically in media containing organic molecules as compared to distilled water. The rich proteose-peptone media described by Schultz (1997) [18] was modified by complete reduction of protein content.

The exposure concentrations used in our experiments (0.1, 1, 10, 100, 1000 μg/ml) were higher than those predicted to be found in the environment [38] [39] and consequently, we were able to conclude

that TiO_2 particles at levels to be expected in the environment pose little threat to a protozoan *T. thermophila*.

CONCLUSIONS

Our results show that effects of nano- and bulk TiO_2 particles in exposure concentrations ranging from 0.1, 10, to 1000 µg/ml result in acclimation of a protozoan *T. thermophila* by its changing its membrane composition in a manner associated with increased membrane rigidity. This study is the first nanoparticle - related study successfully employed fatty acid profiling in eukaryotic cells to elucidate the acclimation response to suspended particles, independent of oxidative stress. In *T. thermophila* cultures treated with TiO_2 concentrations above 10 µg/ml, we have observed a deliberate filling of TiO_2 particles into food vacuoles, and this is followed by clearing. The expected environmental concentrations of TiO_2 particles do not pose a threat to a protozoan *T. thermophila* but chronic exposure may result in undesirable effects on protozoans. The novelty of this study is the finding that changed fatty acid profile lead to increased membrane rigidity while exposure of *T. thermophila* is not accompanied by cytotoxicy. This is a proof that cell - TiO_2 particle interactions are also independent of ROS and oxidative stress.

4 FIGURES

Fig. 1. Experimental arrangement. Three major toxicity endpoints were studied: changes in cell membrane, viability and physiological responses of *T. thermophila* to different exposure concentrations of TiO_2 particles. The culture of *T. thermophila* was preincubated in the PM for 24 hours before beginning the exposure to TiO_2. Changes in membrane composition were assessed by FAME-s method (at 0.1, 10 and 1000 µg TiO_2/ml) and by the extent of lipid peroxidation (measuring MDA content). Viability was assessed by ATP concentration. Two physiological biomarkers distinctive

of *T. thermophila*, namely filling of TiO_2 particles in food vacuoles and cell rupture were also assessed as described by Dai et al. (2008) [24].

Fig. 2. Food vacuoles filled with particles were first visible under a light microscope after four hours at exposure concentrations higher than 10 µg/ml of TiO_2 (A). Control cells with visible vacuoles, however were not filled with dark matter (TiO_2) (B).

Fig. 3. Zeta potentials of TiO_2 nanoparticle suspensions (1000 µg/ml) measured in the nutrient poor medium and used in experimental exposures to living cells.

Fig. 4. Changes of straight chain saturated and unsaturated fatty acids in *T. thermophila* after exposure to different concentrations of TiO_2 at 32°C after 24 h. Bars represent the standard deviation. * Indicates significant differences of straight chain fatty acids from control values ($p < 0.05$). B (bulk concentration), NP (nanoparticle concentration).

Fig. 5. Changes of portions of *iso* and *ante-iso* branched fatty acids in *T. thermophila* at 32°C after 24 h. Bars represent standard deviation. * Indicates significant differences from control values ($p < 0.05$). B (bulk concentration), NP (nanoparticle concentration).

Fig. 6.

Variation of ATP concentration (measured in µmol/l) in cultures *of T. thermophila* exposed to TiO_2 for 24 h at 32°C in one of the two independent assays. The results are expressed as a percentage compared to time (h) of exposure to TiO_2 particles (100% viability). Values were calculated from the averages of three subsamples, standard deviations are given. B (bulk concentration), NP (nanoparticle concentration).

Fig. 7. The percentage of cells containing food vacuoles filled with TiO_2 after exposure of *T. thermophila* to different nano- and bulk TiO_2 exposure concentrations. Data are means of three independent assays. Standard deviations are given. B (bulk concentration), NP (nanoparticle concentration).

5 TABLES

Table 1. Percentage composition of membrane fatty acid samples from *T. thermophila* exposed to TiO_2 particles at 32°C after 24 h. The data are presented as total sums of different types of fatty acids of lipid extracted from the three independent cultures. Percentages are expressed as means ± standard deviation (SD). B (bulk concentration), NP (nanoparticle concentration), FA (fatty acid).

6 REFERENCES

[1] W.H. Suh, K.S. Suslick, G.D. Stucky, Y.H. Suh, Nanotechnology, nanotoxicology, and neuroscience, Prog Neurobiol, 87 (2009) 133-170.
[2] A. Menard, D. Drobne, A. Jemec, Ecotoxicity of nanosized TiO_2. Review of *in vivo* data, Environ Pollut, 159 (2011) 677-684.
[3] S. Singh, T. Shi, R. Duffin, C. Albrecht, D. van Berlo, D. Hohr, B. Fubini, G. Martra, I. Fenoglio, P.J. Borm, R.P. Schins, Endocytosis, oxidative stress and IL-8 expression in human lung epithelial cells upon treatment with fine and ultrafine TiO_2: role of the specific surface area and of surface methylation of the particles, Toxicol Appl Pharmacol, 222 (2007) 141-151.
[4] Y. Shi, J.H. Zhang, M. Jiang, L.H. Zhu, H.Q. Tan, B. Lu, Synergistic genotoxicity caused by low concentration of titanium dioxide nanoparticles and p,p'-DDT in human hepatocytes, Environ Mol Mutagen, 51 (2010) 192-204.
[5] M.M. Banaszak, Nanotoxicology: a personal perspective., Wiley Interdisciplinary Reviews: Nanomedicine and Nanobiotechnology, 1 (2009).
[6] L. Peng, D. Wenli, W. Qisui, L. Xi, The envelope damage of *Tetrahymena* in the presence of TiO_2 combined with UV light, Photochem Photobiol, 86 (2010) 633-638.
[7] M. Mortimer, K. Kasemets, M. Vodovnik, R. Marinsek-Logar, A. Kahru, Exposure to CuO nanoparticles changes the fatty acid composition of protozoa *Tetrahymena thermophila*, Environ Sci Technol, 45 (2011) 6617-6624.
[8] A.P. Bearden, G.D. Sinks, W.H. Vaes, E. Urrestarazu Ramos, J.L. Hermens, T.W. Schultz, Bioavailability, biodegradation, and acclimation of *Tetrahymena pyriformis* to 1-octanol, Ecotoxicol Environ Saf, 44 (1999) 86-91.
[9] T.W. Schultz, G.D. Sinks, A.P. Bearden-Lowit, Population growth kinetics and bulk membrane lipid alterations in *Tetrahymena pyriformis*: exposure to pentachlorophenol, Cell Biol Toxicol, 18 (2002) 271-278.
[10] A.L. Shug, C. Elson, E. Shrago, Effect of iron on growth, cytochromes, glycogen and fatty acids of *Tetrahymena pyriformis*, J Nutr, 99 (1969) 379-386.
[11] J. Fang, D.Y. Lyon, M.R. Wiesner, J. Dong, P.J. Alvarez, Effect of a fullerene water suspension on bacterial phospholipids and membrane phase behavior, Environ Sci Technol, 41 (2007) 2636-2642.
[12] C. Baysse, F. O'Gara, Role of Membrane Structure During Stress Signalling and Adaptation in *Pseudomonas*, Pseudomonas, 2 (2007).
[13] M. Vodovnik, M. Bistan, M. Zorec, R. Marinsek-Logar, Methyl mercury inhibits growth and induces memb rane changes in *Pseudomonas putida*, Acta argiculturae Slovenica, http://aas.bf.uni-lj.si/zootehnika/96-2010/PDF/96-2010-2-87-93.pdf, 96/2 (2010).
[14] M. Vodovnik, A. Levart, R. Marinsek-Logar, Toxicolipidomic approach to detection of mercury compounds with microorganisms, Microbiology for today: book of abstracts Slovenian Microbiological Society, (2008).
[15] Y. Kameyama, S. Yoshioka, Y. Nozawa, Mechanism for adaptive modification during cold acclimation of phospholipid acyl chain composition in *Tetrahymena*. I. Principal involvement of deacylation-reacylation, Biochim Biophys Acta, 793 (1984) 28-33.
[16] A.P. Bearden, B.W. Gregory, T.W. Schultz, Population growth kinetics of *Tetrahymena pyriformis* exposed to selected nonpolar narcotics, Arch Environ Contam Toxicol, 33 (1997) 401-406.
[17] R. Clarke, H.W. van den Berg, R.F. Murphy, Reduction of the membrane fluidity of human breast cancer cells by tamoxifen and 17 beta-estradiol, J Natl Cancer Inst, 82 (1990) 1702-1705.
[18] T.W. Schultz, TETRATOX: *Tetrahymena pyriformis* population growth impairment endpoint-A surrogate for fish lethality., Toxicol. Methods 7(1997) 289-309.
[19] C. Ortega-Villasante, R. Rellan-Alvarez, F.F. Del Campo, R.O. Carpena-Ruiz, L.E. Hernandez, Cellular damage induced by cadmium and mercury in *Medicago sativa*, J Exp Bot, 56 (2005) 2239-2251.
[20] A. Zrimec, Application of the electroconformational coupling model in the study of membrane protein behaviour in oscillating electric fields,

http://cobiss.izum.si/scripts/cobiss?command=DISPLAY&base=COBIB&RID=838223, PhD thesis (2001) 152.
[21] A. Thore, S. Ansehn, A. Lundin, S. Bergman, Detection of bacteriuria by luciferase assay of adenosine triphosphate, J Clin Microbiol, 1 (1975) 1-8.
[22] J. Valant, D. Drobne, K. Sepcic, A. Jemec, K. Kogej, R. Kostanjsek, Hazardous potential of manufactured nanoparticles identified by *in vivo* assay, J Hazard Mater, 171 (2009) 160-165.
[23] E. London, Lipid bilayer structure, Encyclopedia of Biological Chemistry, 2 (2004).
[24] J. Dai, C.-L. Li, Y.-Z. Zhang, Q. Xiao, K.-L. Lei, Y. Liu, Bioenergetic Investigation of the Effects of La(III) and Ca(II) on the Metabolic Activity of Tetrahymena thermophila BF5 Biological Trace Element Research, 122 (2008).
[25] M. Sinensky, Homeoviscous Adaptation—A Homeostatic Process that Regulates the Viscosity of Membrane Lipids in *Escherichia coli*, Proc. Nat. Acad. Sci. USA, 71 (1973).
[26] W. Klein, M.H. Weber, M.A. Marahiel, Cold shock response of *Bacillus subtilis*: isoleucine-dependent switch in the fatty acid branching pattern for membrane adaptation to low temperatures, J Bacteriol, 181 (1999) 5341-5349.
[27] T. Satyanarayana, B.N. Johri, Microbial diversity: current perspectives and potential applications, in: I. K. International Publishing House Pvt, 2005.
[28] T. Ivancic, M. Vodovnik, R. Marinsek-Logar, D. Stopar, Conditioning of the membrane fatty acid profile of *Escherichia coli* during periodic temperature cycling, Microbiology, 155 (2009) 3461-3463.
[29] C. Laroche, L. Beney, P.A. Marechal, P. Gervais, The effect of osmotic pressure on the membrane fluidity of *Saccharomyces cerevisiae* at different physiological temperatures, Appl Microbiol Biotechnol, 56 (2001) 249-254.
[30] A. Alonso, C.S. Queiroz, A.C. Magalhaes, Chilling stress leads to increased cell membrane rigidity in roots of coffee (*Coffea arabica L.*) seedlings, Biochim Biophys Acta, 1323 (1997) 75-84.
[31] W. Pauli, S. Berger, Toxicological comparisons of *Tetrahymena* species, end points and growth media: supplementary investigations to the pilot ring test, Chemosphere, 35 (1997) 1043-1052.
[32] S.M. Hussain, K.L. Hess, J.M. Gearhart, K.T. Geiss, J.J. Schlager, In vitro toxicity of nanoparticles in BRL 3A rat liver cells, Toxicol In Vitro, 19 (2005) 975-983.
[33] C.M. Sayes, D.B. Warheit, An *in vitro* investigation of the differential cytotoxic responses of human and rat lung epithelial cell lines using TiO_2 nanoparticles, International Journal of Nanotechnology 5(2008) 15-29.
[34] J.R. Gurr, A.S. Wang, C.H. Chen, K.Y. Jan, Ultrafine titanium dioxide particles in the absence of photoactivation can induce oxidative damage to human bronchial epithelial cells, Toxicology, 213 (2005) 66-73.
[35] H. Wang, R.L. Wick, B. Xing, Toxicity of nanoparticulate and bulk ZnO, Al_2O_3 and TiO_2 to the nematode *Caenorhabditis elegans*, Environ Pollut, 157 (2009) 1171-1177.
[36] M. Mortimer, K. Kasemets, A. Kahru, Toxicity of ZnO and CuO nanoparticles to ciliated protozoa *Tetrahymena thermophila*, Toxicology, 269 (2010) 182-189.
[37] R.C. Murdock, L. Braydich-Stolle, A.M. Schrand, J.J. Schlager, S.M. Hussain, Characterization of nanomaterial dispersion in solution prior to *in vitro* exposure using dynamic light scattering technique, Toxicol Sci, 101 (2008) 239-253.
[38] N.C. Mueller, B. Nowack, Exposure modeling of engineered nanoparticles in the environment, Environ Sci Technol, 42 (2008) 4447-4453.
[39] K. Tiede, A.B. Boxall, S.P. Tear, J. Lewis, H. David, M. Hassellov, Detection and characterization of engineered nanoparticles in food and the environment, Food Addit Contam Part A Chem Anal Control Expo Risk Assess, 25 (2008) 795-821.

Table 1

Particle type		Bulk (B)			Nanoparticles (NP)		
Particle concentration (µg TiO_2 /ml)	**0**	**0.1**	**10**	**1000**	**0.1**	**10**	**1000**
Unsaturated FA (%)	**48.9±2.5**	**48.6±3.2**	**44.3±2.5**	**44.5±3.9**	**41.8±3.1**	**42.7±2.2**	**42.8±2.2**
- monounsaturated FA (1x) (%)	16.3 ±2.5	18.6±3.3	18.5±2.8	18.2±1.6	23.5±2.9	24.7±2.3	23.0±2.0
- polyunsaturated FA (2x) (%)	8.6±0.8	8.1±0.6	10.0±0.5	8.5±0.3	9.7±0.2	9.3±0.3	11.1±0.2
- polyunsaturated FA (3x) (%)	19.0±4.1	17.6±0.4	19.1±1.3	19.6±2.0	18.4±1.0	17.5±1.6	16.2±0.9
Saturated FA (%)	**47.8±3.1**	**47.5±4.2**	**44.3±3.5**	**44.5±1.9**	**41.8±2.7**	**42.7±2**	**42.8±3.1**
Straight chain saturated FA(%)	**23.1 ± 3.6**	**42.0±4.9**	**39.6±4.1**	**39.0±2.4**	**37.9±2.6**	**38.4±2.0**	**38.1±3.1**
Branched chain *iso* and *anteiso* saturated FA (%)	**24.7±3.5**	**6.5±0.7**	**4.7±1.1**	**5.5±0.6**	**3.9±0.6**	**4.3±0.6**	**4.7±0.5**
- saturated *iso* FA (%)	8.6±1.1	5.8±0.7	4.6±0.7	5.1±0.5	3.7±0.7	4.1±0.8	4.5±0.6
- saturated *anteiso* FA (%)	16.1±0.2	0.7±0.1	0.1±0.2	0.3±0.1	0.1±0.0	0.2±0.0	0.3±0.0
Average number of C-atoms in membrane FA	**15.3**	**16.0**	**15.9**	**15.5**	**16.1**	**16.2**	**16.0**

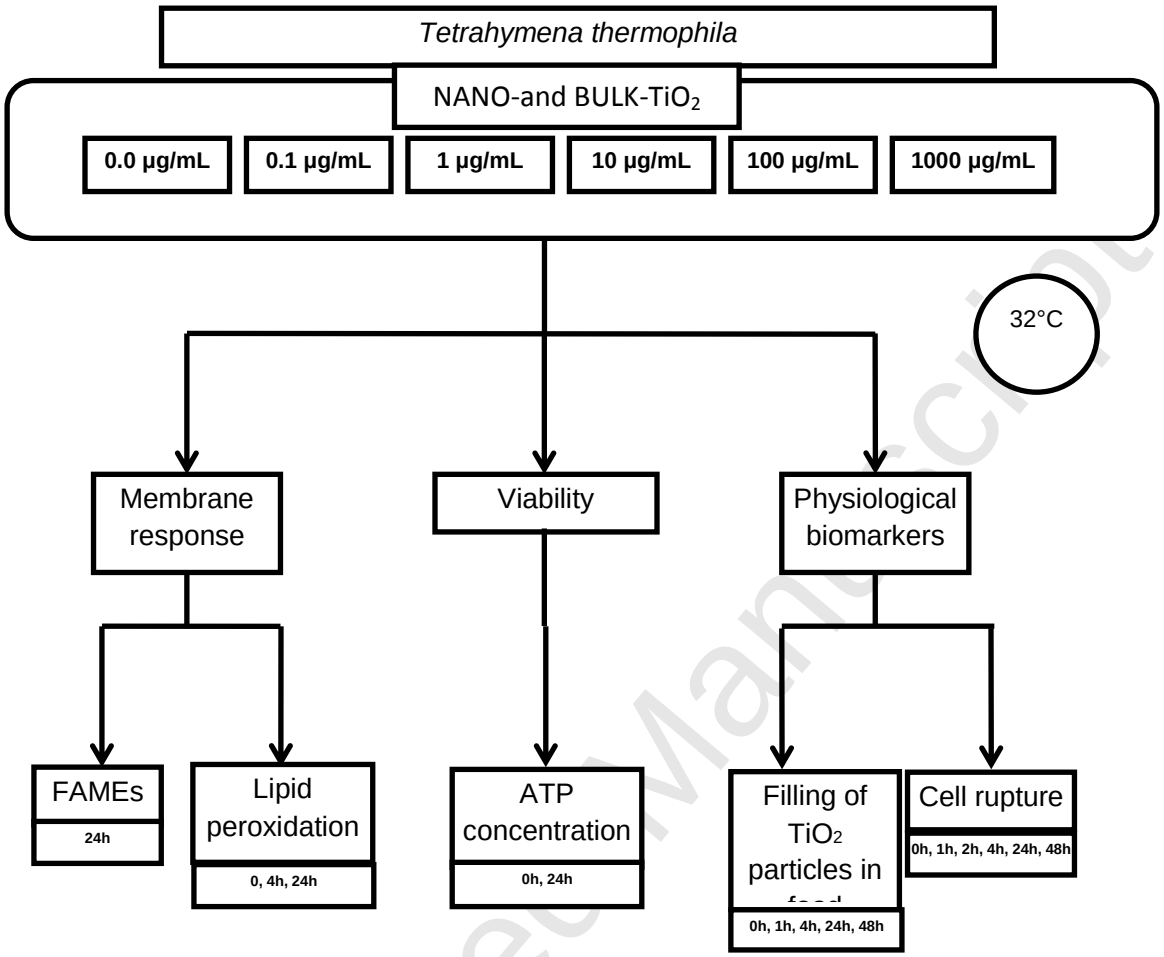

Fig. 1.

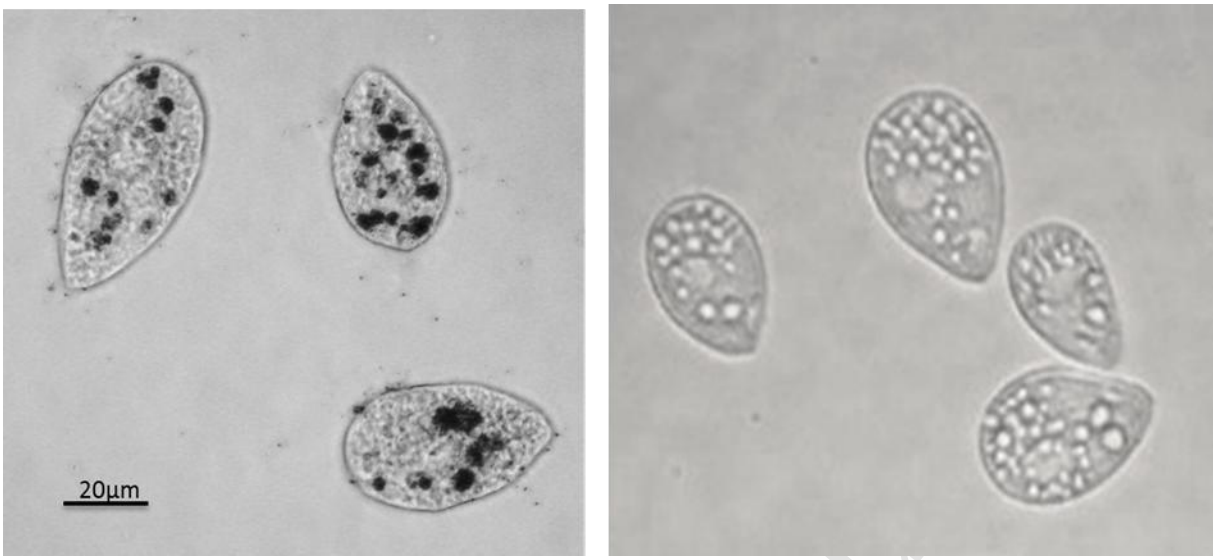

A **B**

Fig. 2.

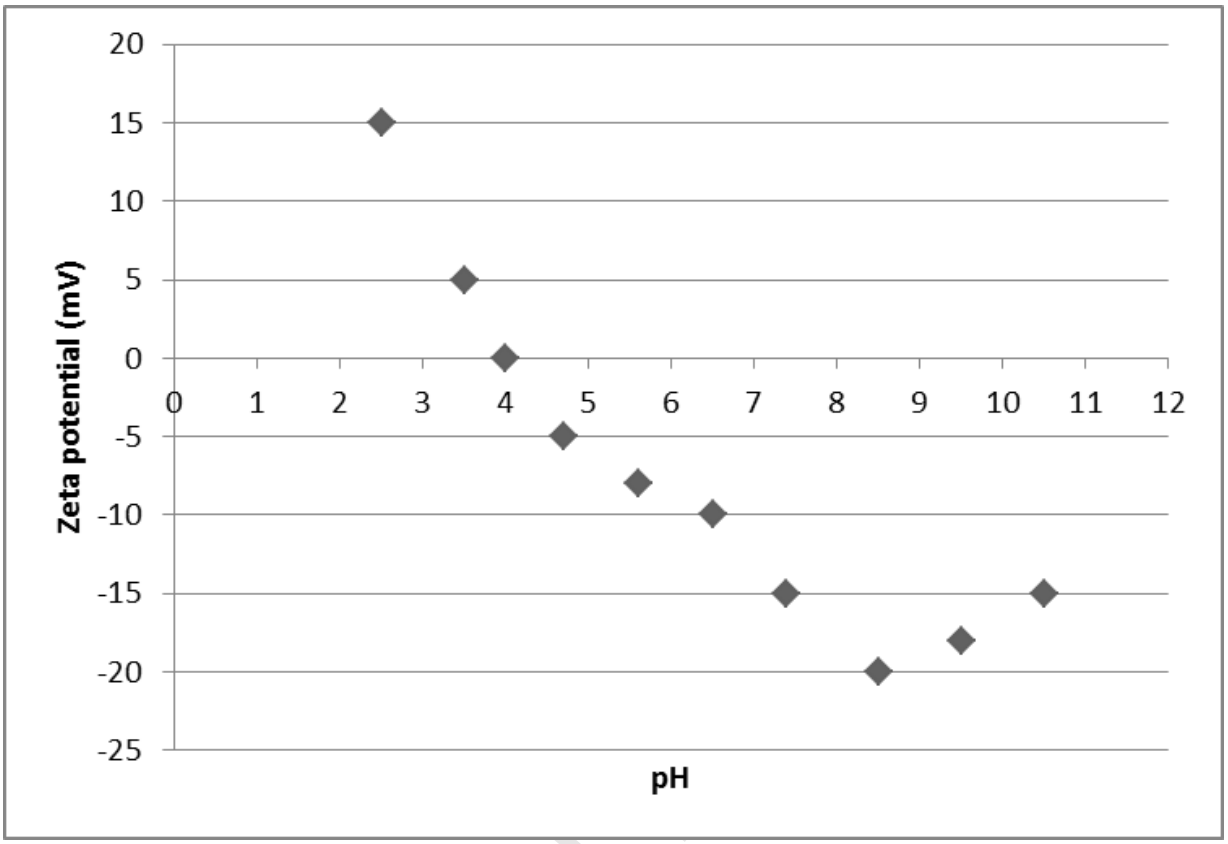

Fig. 3.

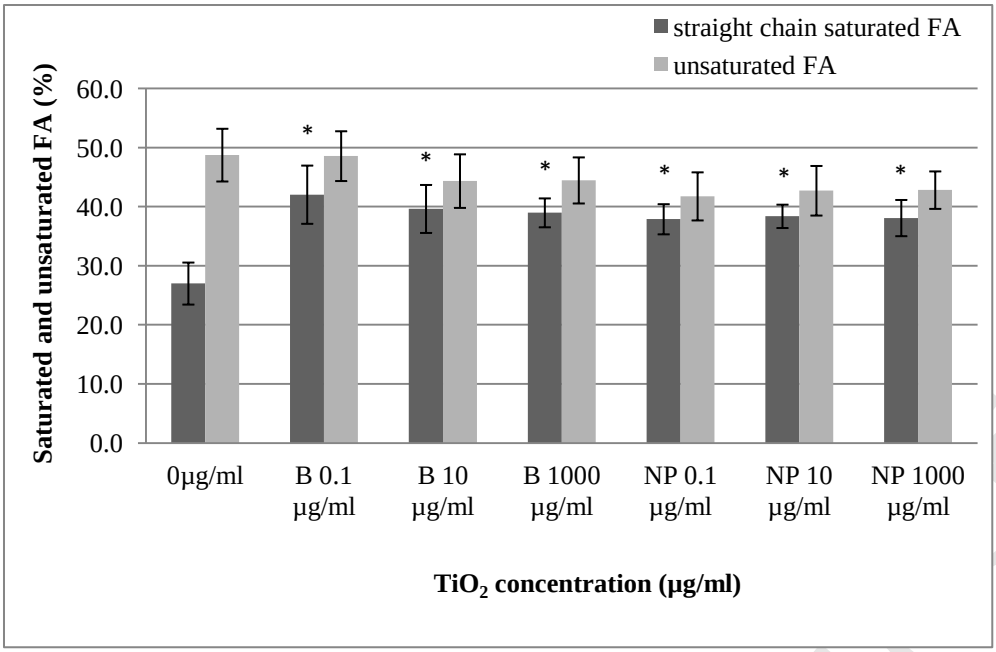

Fig. 4

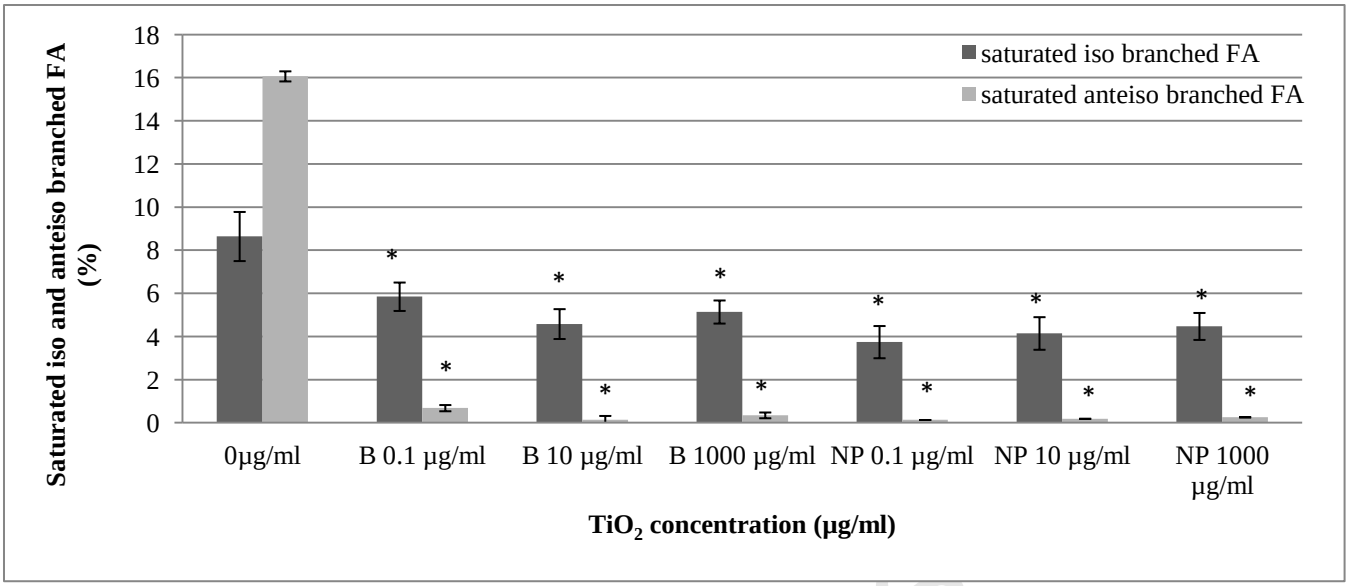

Fig. 5

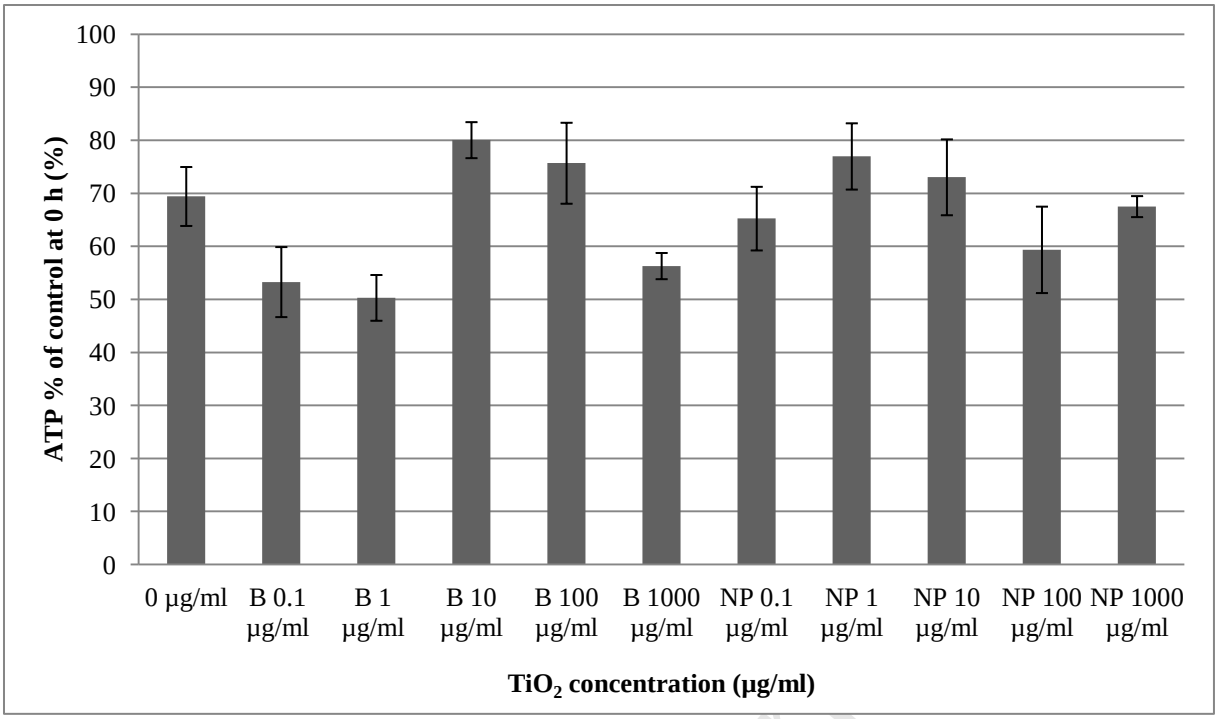

Fig. 6.

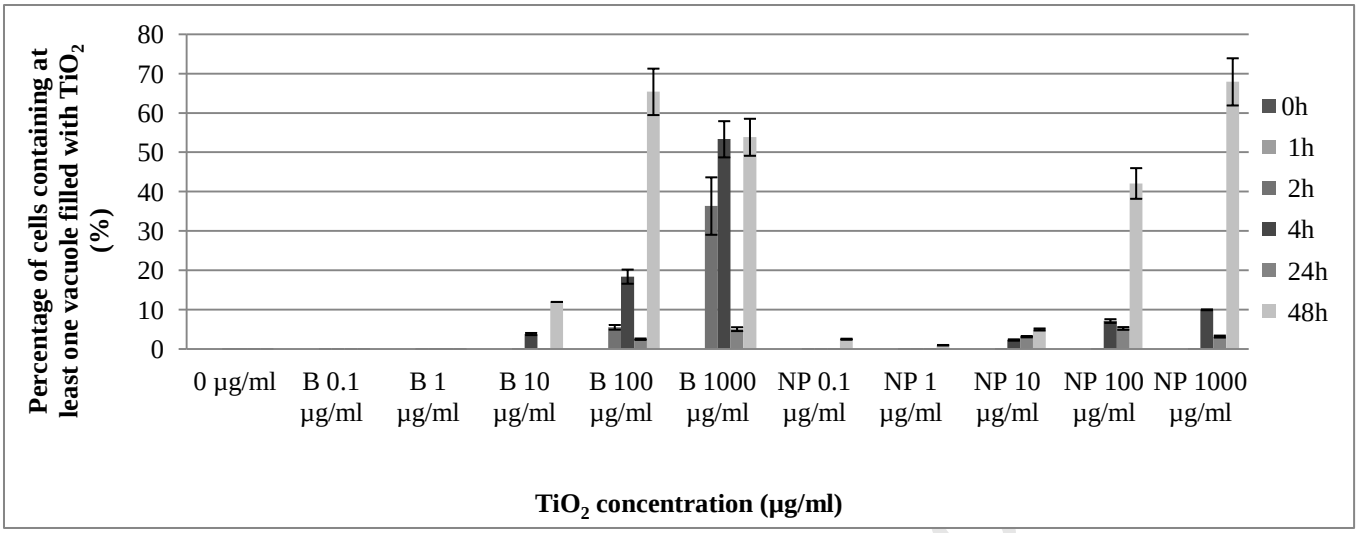

Fig. 7